Uplink Dimensioning Over Log-Normal Shadowing for OMA and NOMA Schemes

Bin Liu, Philippe Martins, Laurent Decreusefond, Jean-Sebastien Gomez, Rongfang Song

Uplink Dimensioning Over Log-Normal Shadowing for OMA and NOMA Schemes

Bin Liu, Philippe Martins, Laurent Decreusefond, Jean-Sebastien Gomez, and Rongfang Song

***Abstract*—This paper investigates the uplink dimensioning problem for OMA (Orthogonal Multiple Access) and NOMA (Non-Orthogonal Multiple Access) schemes. Dimensioning is to make radio resource provision for a service area to fulfill an outage constraint. The radio resource limit and outage in dimensioning make classical inhomogeneous Poisson assumption of uplink served user point process questionable. In this paper, we first prove that this process admits a homogeneous Poisson distribution in the limiting regime. As a consequence, uplink coverage probabilities over log-normal shadowing for both schemes are derived. Then, tractable stochastic geometry models for two schemes are proposed to obtain numbers of total required radio blocks. Their upper bounds under an outage constraint are also given to reduce computing overhead. Finally, the simulations confirm accuracy of derivations and demonstrate the effectiveness of our models.**

***Index Terms*—Network Dimensioning, Stochastic Geometry, OMA, NOMA, Log-normal Shadowing.**

I. Introduction

The fifth generation cellular network supports low delay, high throughput, and massive mobile user/device accesses. To achieve these targets, telecommunication operators shall carefully assign proper radio resources to guarantee high Quality-of-Service (QoS) for the user equipment (UE) in their service areas, such as in airports, in office buildings, in business centers. A natural question arises: for a required overloading probability, how many radio resources shall be assigned to base stations (BSs) in these service areas? Alternatively, given radio resources in these BSs, what is the acceptable UE loads. This is a network dimensioning problem, and becomes indispensable in recent years with ever-increasing UE data demands.

There have been several studies on dimensioning problems. An early research [1] investigated user performance, such as blocking probability and throughput, for classical cellular networks. Reference [2] studied dimensioning of orthogonal frequency division multiple access in noise-limited downlink networks. This work was extended to fast fading cases for downlink networks in [3]. Blaszczyszyn [4] derived coverage probability in downlink direction for infinite log-normal shadowing networks. Because of the coupling of interference and traffic, Karray [5] used queuing theory to characterize network parameter dimensioning. All aforementioned works have not considered uplink dimensioning over shadowing.

In recent years, the enormous wireless throughput demands motivate the NOMA application. Saito [6] first proposed the NOMA scheme in power domain in dowinlink direction. Zhang [7] expanded NOMA to uplink direction through analyzing the outage and sum-rate performance. Afterwards, a stochastic geometry (SG) model was employed to demonstrate the system wide NOMA performance gains over OMA in [8], where the uplink power control scheme in [9] was adopted. This classical scheme in [8] [9] was expanded to over-compensation and enhancement power controls for the NOMA scheme in [10]. In [11], a network NOMA scheme was proposed to realize uplink coordinated multi-point transmission to further improve coverage and ergodic rates. In the recent work [12], Wei systematically compared the ergodic rate gain of NOMA over OMA in uplink direction for various network scenarios. A related NOMA capacity dimensioning work in [13] studied the classical user pairing problem. Unfortunately, these prior literature on NOMA focused only on the physical layer in the network without shadowing.

In recognition of these facts, employing SG to investigate dimensioning for NOMA scheme in uplink direction becomes indispensable for 5G and beyond. Roughly speaking, SG analysis for dimensioning faces the following challenges: (1) The inhomogeneous Poisson assumption of uplink user point process (p.p.) applied in existing literature can not be reused directly because of resource limitation effect in the context of dimensioning. (2) How the shadowing effect impacts dimensioning is still an open issue. Motivated by above facts, we first investigate uplink served user p.p. distribution. Then, the SG dimensioning models for both OMA and NOMA schemes are derived in the shadowing network. To the best of our knowledge, this paper is the first work on these issues.

Our contributions are threefold. *Firstly*, we prove that the uplink served user p.p. admits homogeneous Poisson distribution. *Secondly*, uplink SG models of two schemes are derived to obtain expressions of total required Radio Block (RB) numbers. We also give their upper bounds to simplify network deployment. *Thirdly*, simulation results confirm the homogeneous Poisson assumption, and the effectiveness of SG models in determining RB provisions. Incidentally, since the terms UE and user have the same meaning in this paper, hereafter, they will be used interchangeably.

II. System Model

We consider an interference-limited uplink cellular network, where the wireless channel in each BS is sliced in a grid of RBs. In a service area, the BSs and UEs are deployed according to homogeneous Poisson point processes Φ_b with intensity λ_b, and Φ with intensity λ respectively. Since we investigate uplink dimensioning, we assume $\lambda \gg \lambda_b$, namely the network is saturated. Each BS-UE link has independent and identically distributed (i.i.d.) log-normal shadowing S_i, $i \in \mathbb{N}$. A UE selects the BS with minimal propagation loss (including path-loss and shadowing) as its serving BS. Hence, all UEs camping on the same BS form a "virtual" cell. On

This work was supported in part by Jiangsu Government Scholarship for Overseas Studies under Grant JS-2018-7, and in part by the Open Research Fund of Key Lab of Broadband Wireless Communication and Sensor Network Technology, NJUPT, Ministry of Education, under Grant JZNY201906.

Bin Liu, Rongfang Song are with the School of Telecommunication and Information Engineering, Nanjing University of Posts and Telecommunications (NJUPT), China. (e-mail: liubin0430, songrf@njupt.edu.cn).

Philippe Martins, Laurent Decreusefond, Jean-Sebastien Gomez are with Computer Sciences and Networks (INFRES) Department, TELECOM ParisTech, France (e-mail: martins, laurent.decreusefond, jgomez @telecom-paristech.fr).

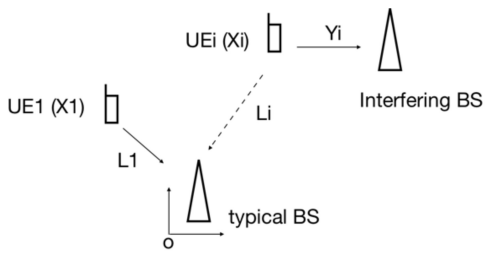

Fig. 1: System model in uplink OMA scheme.

one RB in the OMA scheme, each BS uniformly selects one UE in its "virtual" cell to provide uplink service. All UEs utilize distance-shadowing based total power control strategy to compensate the large-scale propagation loss. In OMA scheme, we assume: 1) all the UEs have the same uplink transmission data rate requirements. 2) and all the UEs have the same target received power P_u at their serving BSs. Without loss of generality, the performance analysis is performed at the typical BS at origin thanks to Slivnyak's theorem [14]. A UE camping on this typical BS on one RB is referred to as the typical UE at location x_1, as shown in Fig.1.

The served user p.p. distribution is a key prerequisite in a SG model. In most literature, uplink user p.p. is usually assumed to admit Poisson distribution. M. Haenggi [15] showed that this p.p. is an inhomogeneous Poisson process. At the same year, an approximation of uplink user p.p. was given in [16] to reduce computation consumption. Afterwards, exact uplink user p.p. distribution in [15] is leveraged to obtain Signal-to-Interference Ratios (SIR) meta distribution in [17] in a network with power control. These classical uplink analyses are based on the assumption of ideal network with unlimited radio resource. In the context of dimensioning, the practical limited radio resource in a saturated network leads to service outage, namely not all users are served or not all RB requirements are satisfied. As a result, the classical Poissoness of uplink served user p.p. demands re-investigation. The following lemma 1 shows that it approaches a homogeneous Poisson p.p. in the limiting regime. Therefore, in OMA scheme, the collection of all UEs on one RB served by different BSs is assumed to be a homogeneous Poisson p.p. $\Phi_u = \{x_i\}_{i\in\mathbb{N}}$ with intensity λ_u.

Lemma 1: Assume that both BS and UE point processes admit homogeneous Poisson distributions with intensities λ_b and λ respectively, and each BS has limited radio resource, under the condition of $\lambda \gg \lambda_b$, the served uplink UE p.p. approaches a homogeneous Poisson p.p. as $\lambda -> \infty$ in the networks without shadowing or with weak shadowing.

Proof: Without loss of generality, we assume $\lambda_b = 1$, and there are M $(M \in \mathbb{N}, M < \lambda)$ RBs to be allocated per BS to M UEs of one-RB requirement. A simple uplink network model is considered: each BS picks an UE uniformly among its M closest UEs on one RB.

In the network without shadowing and fading, the square of the radius of the inscribed circle into the typical Voronoi cell, denoted by R_I^2, has an exponential distribution of parameter $4\pi\lambda_b$ [18]. The M-th farthest point of a Poisson p.p. from a given point is located at a distance whose square, denoted by R_M^2, has a gamma distribution of parameters M and $\pi\lambda$. A very conservative event that guarantees the typical Voronoi cell contains M points, has the probability

$$\mathbb{P}(R_M^2 \leq R_I^2) = \left(\frac{\pi\lambda}{\pi\lambda + 4\pi\lambda_b}\right)^M \tag{1}$$

This probability goes to 1 when λ goes to infinity. It shows when $\lambda \gg \lambda_b$, the M closest UEs to a given BS are within its Voronoi cell with a high probability. We can even let M go to infinity with λ provided that we keep $M = o(\lambda)$.

Next, consider the case that a BS picks an UE uniformly among its M closest UEs. From the previous considerations, the situation at each BS is similar and is independent of the situation at the other BSs. For a BS located at y, the uniformly chosen UE among M UEs is located at a point $x(y) = y + Re^{i\theta}$, where R and θ are independent random variables. The distribution of θ is uniform over $[0, 2\pi)$ and the distribution of R^2 is

$$f_{R^2}(r) = \sum_{j=1}^{M} \frac{1}{M} \frac{(\pi\lambda)^j}{(j-1)!} r^{j-1} e^{-\pi\lambda r} \tag{2}$$

The displacement theorem [14] entails that $\Phi_u = \{x(y),\, y \in \Phi_b\}$ is a Poisson p.p. because of the situation independence at each BS. Since the distribution of $x(y) - y$ is independent of the location y, the p.p. Φ_u is stationary hence it is homogeneous. As we have as many points in Φ_b as in Φ_u, the intensity of Φ_u is λ_b.

In the network with strong shadowing, the previous reasoning does not hold any longer because the shape of the domain monitored by a given BS is totally unknown. However, considering the fact that weak shadowing slightly perturbs the UE location distribution, we can still approximate Φ_u by a homogeneous Poisson p.p. of intensity $\lambda_u = \lambda_b$.

■

Remark 1: Lemma 1 gives an insight on what happens when intensity of UE p.p. approaches infinity. With lemma 1 at hand, we can safely take advantage of tractability of Poisson p.p. to analyze network performance in the context of dimensioning.

III. Uplink Coverage Performance

In order to make this paper self-contained, in the following, we derive uplink coverage probability briefly. The path-loss function is modeled by $\ell(x) = (K|x|)^\beta$ with constant $K > 0$ and path-loss exponent $\beta > 2$. Let $S = \exp(m + \sigma N)$ to represent shadowing variable, where N is the standard Gaussian random variable with zero mean and unit variance. To simplify the analysis, let $\mathbb{E}[S] = 1$ [4]. Define propagation loss between UE x_i, $x_i \in \Phi_u$ and the typical BS as $L_i \triangleq \ell(x_i)/S(x_i)$, where $S(x_i)$ is their link shadowing. Also define Y_i as the propagation loss between UE x_i and its serving BS (see Fig.1). Then, the received power P_i, $i \in \mathbb{N}$ on the typical BS from each UE x_i becomes $P_i = P_u Y_i / L_i$. Note that Y_i, $i \in \mathbb{N}$ are i.i.d. and can be represented by random variable Y. It has Cumulative Distribution Function (CDF) [4]: $F_Y(y) = 1 - \exp(-by^{2/\beta})$, where $b \triangleq \lambda_b \pi \mathbb{E}(S^{2/\beta})/K^2$. We further define propagation loss process as $\Theta_u \triangleq \{L_i\}_{i\in\mathbb{N}}$. Following

the same line as in [4], one can obtain that the propagation loss process Θ_u is inhomogeneous Poisson p.p. with intensity measures $\Lambda_a([0,\ t)) = at^{2/\beta}$, where $a \triangleq \lambda_u \pi \mathbb{E}(S^{\frac{2}{\beta}})/K^2$.

In order to find the interfering power distribution, we also define a relative propagation loss process as $\Psi \triangleq \{\frac{L_i}{Y}\}_{i\in\mathbb{N}} = \{H_i\}_{i\in\mathbb{N}}$, where H_i is the relative propagation loss from UE x_i to the typical BS. Note that $H_1 = 1$, while $H_i > 1$, $i \in \mathbb{N}\backslash\{1\}$. With these parameter definitions, we can derive interfering power distribution by inspecting the intensity measure of relative propagation loss process Ψ, as shown in lemma 2.

Lemma 2: The relative propagation loss process Ψ is inhomogeneous Poisson p.p. on $(1, +\infty)$ with intensity measure $\Lambda((1,\ h)) = h^{\frac{2}{\beta}} - 1, \quad h \in (1, +\infty)$.

Proof: The p.p. Ψ can be viewed as a transformation of p.p. Θ_u by the probability kernel

$$p(t,\ A) = \mathbb{P}\left\{\frac{t}{Y} \in A\right\},\ t \in (0,\ +\infty),\ A \in \mathcal{B}(\mathbb{R}^+)$$

In terms of the displacement theorem [14], when $h \in\ (1,\ +\infty)$, the Ψ is Poisson p.p. with intensity measure:

$$\Lambda((1,h)) = \int_0^{+\infty} p(t,\ (1,h))\,\Lambda_a(dt) = h^{2/\beta} - 1$$

where the $\lambda_b = \lambda_u$ is used in the last equation. ■

Remark 2: Thanks to homogeneous served UE Poisson p.p. in the limiting regime, the distribution of Ψ as well as coverage probability (see below), are invariant with respect to both the shadowing effect and intensities of BS and UE point processes, on the condition that both uplink and downlink suffer from shadowing effects of the same distribution.

Then, sum of interference power $I = \sum_{h_i>1}^{+\infty} \frac{1}{h_i}$ has the Laplace transform

$$\begin{aligned}\mathcal{L}_I(z) = \mathbb{E}[e^{-zI}] &= \exp\{-\int_1^{+\infty}(1 - e^{-\frac{z}{h}})\Lambda(dh)\} \\ &= \exp(1 - \varphi_\beta(z)),\ z \in \mathbb{R}^+ \end{aligned} \tag{3}$$

where $\varphi_\beta(z) \triangleq e^{-z} + z^{\frac{2}{\beta}}\gamma(1-\frac{2}{\beta}, z)$, and $\gamma(\alpha, z) = \int_0^z t^{\alpha-1}e^{-t}dt$ is the lower incomplete gamma function.

Finally, coverage probability is written as $P_c(\theta) = \mathbb{P}\{I \le 1/\theta\} = F_I(1/\theta)$, where $F_I(y)$, $(y \in \mathbb{R}^+)$ is the CDF of interference power I. This CDF can be retrieved from numerical inverse Laplace transform of $\frac{1}{z}\mathcal{L}_I(z)$, i.e., $F_I(y) = \mathcal{L}^{-1}\{\frac{1}{z}\mathcal{L}_I(z)\}$. Incidentally, we let $\theta > 1$ ensure only one BS is selected by one UE.

Remark 3: Thanks to the power control mechanism, the coverage probability is only a function of the path-loss component β. As shown in the simulation section, the coverage probability increases and the RB requirement decreases as a consequence of the increasing β.

IV. Uplink Dimensioning

A. OMA Dimensioning

Dimensioning determines the RB provision in a service area for the acceptable UE loads or total RB requirements if an overloading constraint is given. Since UE load can be viewed as a special case of the UE with fixed RB requirement, we focus on the latter case where UEs have variable RB requirements. The outage rate is defined as the mean ratio of the unfulfilled total RB requirements to the total RB requirements in a service area with respect to BS and UE p.p. distributions.

Generally, the total RB provision on BSs is a function of both Φ_b and Φ_u point processes. All BSs allocate RBs of different numbers to different UEs according to their SIRs, which in turn are highly coupled with the UE deployment on every RB. To simplify the analysis, we investigate the mean required RBs, and regard the collection of served UEs on each RB at different BSs as a p.p. realization ϕ_u of Φ_u.

Firstly, the allocated RB number in a BS for a served UE is expressed by

$$n(\phi_u) = \min(\left\lceil \frac{C}{W_{rb} log_2(1 + SIR(\phi_u))} \right\rceil, l_m) \tag{4}$$

where W_{rb} is the bandwidth of one RB; the l_m is the maximum number of RBs that can be allocated to a UE to avoid resource overuse; and the C refers to UE capacity requirement. Thus, the number of total RBs allocated by BS p.p. realization ϕ_b to fulfill all UE requirements in a compact set $A \in \mathbb{R}^2$ is given by

$$N(\phi_b) = \sum\nolimits_{y_j \in \phi_b} \mathbb{E}_{\Phi_u}[n(\phi_u)] = \int_{y\in A} \mathbb{E}_{\Phi_u}[n(\phi_u)]\phi_b(dy) \tag{5}$$

We define θ_l as the required SIR to allocate l RBs to a UE. According to the Shannon formula, the relation between θ_l and capacity C is given by $\theta_l = 2^{C/(l\cdot W_{rb})} - 1$, $l \in\ \{1, 2, \dots l_m - 1\}$ and $\theta_0 = +\infty,\ \theta_{l_m} = -\infty$. Hence, (5) can be rewritten as

$$\begin{aligned} N(\phi_b) &= \int_{y\in A} \mathbb{E}_{\Phi_u}[\sum\nolimits_{l=1}^{l_m} l \cdot \mathbf{1}_{[\theta_l, \theta_{l-1})}\{SIR(\phi_u)\}]\phi_b(dy) \\ &= \sum\nolimits_{l=1}^{l_m} l \int_{y\in A}\int_{\mathcal{N}_u} \mathbf{1}_{[\theta_l,\theta_{l-1})}\{SIR(\phi_u)\}d\mathbb{P}(\phi_u)\phi_b(dy) \end{aligned} \tag{6}$$

where $\mathbf{1}\{\cdot\}$ is an indicator function that equals 1 when the condition in the brace is satisfied and 0 otherwise. The $\mathcal{N}_u$ is UE configuration space, $\mathbb{P}(\cdot)$ is probability measure. Let P_c^l refer to the probability of SIR in region $[\theta_l, \theta_{l-1})$, i.e., $P_c^l \triangleq \mathbb{P}_{\Phi_u}\{\mathbf{1}_{[\theta_l,\theta_{l-1})}\{SIR(\phi_u)\}\}$. Hence, (6) can be simplified to

$$N(\phi_b) = \sum_{l=1}^{l_m} l \int_{y\in A} P_c^l \phi_b(dy) = \sum_{l=1}^{l_m} l\phi_b(A_l) \tag{7}$$

where compact set $A_l \in \mathbb{R}^2$, $|A_l| \triangleq P_c^l|A|$, and $|A_l|$ is a Lebesgue measure. Since the BS p.p. is a Poisson one, $\phi_b(A_l)$ follows a Poisson law of parameter $\lambda_b|A_l|$. Equation (7) shows that given a BS p.p. realization ϕ_b, the mean number of total RBs $N(\phi_b)$ is a compound Poisson process.

Remark 4: The uplink dimensioning (7) seems unrelated to the shadowing effect, but strong shadowing can enhance edge effect and impact the RB provision for a finite service area

(see simulation section for details).

Finally, the expectation of the mean number of total RBs with respect to Φ_b is given by

$$\bar{N}_{tot} = \mathbb{E}_{\Phi_b}\left[\frac{\lambda}{\lambda_b} N\left(\phi_b\right)\right] = \sum_{l=1}^{l_m} l\lambda P_c^l |A|. \tag{8}$$

Given an target outage rate, leveraging (7) to determine imperative total RB provision demands high memory and computing consumption. Whereas an upper bound for the number of total RBs according to concentration inequality [2] [3] can significantly ease network deployment task. For target outage rate $\epsilon > 0$, the upper bound is written as $\hat{N}_{tot} = \bar{N}_{tot} + \alpha$, where α is the root of

$$g\left(\frac{\alpha l_m}{\sum_{l=1}^{l_m} l^2 \lambda P_c^l |A|}\right) = -\frac{l_m^2 \ln(\epsilon)}{\sum_{l=1}^{l_m} l^2 \lambda_b P_c^l |A|} \tag{9}$$

and $g\left(c\right) = (1+c)\ln\left(1+c\right) - c$, for all $c > 0$.

B. NOMA Dimensioning

In uplink direction, each BS selects two UEs on one RB as a NOMA group. Reference [8] pointed out this 2-UE NOMA scheme is more practical because of lower processing complexity. We apply power back-off scheme in [7] [8] to differentiate UEs in a same NOMA group. One of the NOMA UE is selected randomly and is backed off its transmission power by a factor of ρ, $\rho \in (0, 1]$, i.e., the received power on its serving BS becomes ρP_u. This back-off UE is treated as UE2. The left UE in the same NOMA group keeps its receiving power on its serving BS unchanged, i.e., P_u, and is treated as UE1. To simplify the analysis, we also let UE1 collection, or UE2 collection, has the same target received power at their serving BSs. The UE1 and UE2 camping on the typical BS are at locations x_1, x_2 respectively. In addition, the locations of all UE1 and UE2 are assumed to constitute homogeneous Poisson point processes Φ_{u1} and Φ_{u2} respectively, and $x_1 \in \Phi_{u1}$, $x_2 \in \Phi_{u2}$.

We also make following assumptions: (1) The perfect successive interference cancellation processing exists at all BSs. (2) All BSs in a service area can coordinate the resources to minimize the number of total RBs.

Firstly, we define I_1 and I_2 as interferences from Φ_{u1} and Φ_{u2} respectively

$$I_1 = \sum_{i\in\mathbb{N}, x_i \in \Phi_{u1}\setminus\{x_1\}} P_{1,i}, \quad I_2 = \sum_{j\in\mathbb{N}, x_j \in \Phi_{u2}\setminus\{x_2\}} P_{2,j} \tag{10}$$

where $P_{1,i}$ and $P_{2,j}$ respectively are received power of i-th UE1 and j-th UE2 on the typical BS. Based on the NOMA system model, the coverage probabilities for UE1 and UE2 respectively are written as

$$\begin{aligned} P_{c1}\left(\theta\right) \triangleq& \mathbb{P}\left\{\frac{P_u}{\rho P_u + I_1 + I_2} \geq \theta\right\} = \mathbb{P}\left\{I_1 + I_2 \leq 1/\theta - \rho\right\} \\ P_{c2}\left(\theta\right) \triangleq& \mathbb{P}\left\{\frac{P_u}{\rho P_u + I_1 + I_2} \geq \theta, \frac{\rho P_u}{I_1 + I_2} \geq \theta\right\} \\ =& \mathbb{P}\left\{I_1 + I_2 \leq \min(1/\theta - \rho, \rho/\theta)\right\} \end{aligned} \tag{11}$$

Similarly, the CDFs of $P_{c1}\left(\theta\right)$ and $P_{c2}\left(\theta\right)$ can be achieved through the Laplace transform $\mathcal{L}_{I_1+I_2}\left(z\right)$ of the interference summation $I_1 + \ I_2$. Then, the probabilities for UE1 and UE2 when SIRs are in region $[\theta_l, \theta_{l-1})$ are expressed respectively by P_{c1}^l and P_{c2}^l. In this way, the expectations of mean numbers of total RBs for UE1 and UE2 collections respectively are given by

$$\bar{N}_{tot1} = \sum_{l=1}^{l_m} l\lambda P_{c1}^l \left|A\right|/2, \quad \bar{N}_{tot2} = \sum_{l=1}^{l_m} l\lambda P_{c2}^l \left|A\right|/2 \tag{12}$$

We can leverage upper bounds to simplify network deployment in the same way. For target outage rate $\epsilon > 0$, these upper bounds for UE1 and UE2 collections are expressed respectively by $\hat{N}_{tot1} = \bar{N}_{tot1} + \mu$ and $\hat{N}_{tot2} = \bar{N}_{tot2} + \nu$. Here, μ and ν respectively are the roots of

$$\begin{aligned} g\left(\frac{\mu l_m}{\sum_{l=1}^{l_m} l^2 \lambda P_{c1}^l \left|A\right|/2}\right) &= -\frac{l_m^2 \ln(\epsilon)}{\sum_{l=1}^{l_m} l^2 \lambda_b P_{c1}^l \left|A\right|} \\ g\left(\frac{\nu l_m}{\sum_{l=1}^{l_m} l^2 \lambda P_{c2}^l \left|A\right|/2}\right) &= -\frac{l_m^2 \ln(\epsilon)}{\sum_{l=1}^{l_m} l^2 \lambda_b P_{c2}^l \left|A\right|} \end{aligned} \tag{13}$$

Finally, determine the upper bound by $\max\left(\hat{N}_{tot1}, \hat{N}_{tot2}\right)$.

V. Performance Evaluation

In this section, the performance of SIR CDF and number of total RBs are numerically evaluated by extensive Monte Carlo simulation. In the simulation, $P_u = 1W$, $\lambda = 10\lambda_b$, $C = 1Mb/s$, $W_{rb} = 180KHz$, $l_m = 6$ for OMA and $l_m = 9$ for NOMA, target outage rate $\epsilon = 10^{-2}$. In order to mitigate the edge effect, we inspect the central ¼ rectangle of service area. Since the service area is finite, we add an analytical mean interference term in the simulation to represent the mean interference from the outside service area.

Fig.2 demonstrates SIR CDF of BS intensity 20/unit area. It shows that: (1) The simulation and analytical results match well in the network without shadowing and with weak shadowing ($\sigma \leq 6dB$). This validates our homogeneous Poisson assumption of uplink served UE p.p. (2) Increasing path loss exponent β makes the wireless environment harsher and more insensitive to remote interference estimation error. It is worthwhile to remark that the strong shadowing makes served UEs locate outside the service area with a high probability and enhances edge effect. Consequently, simulation curves of high shadowing variances deviate from their analytical results.

Fig. 3(a) shows numbers of total RBs for different shadowing effects and their upper bounds in the OMA scheme. The larger the channel path loss exponent, the less total RBs the service area demands. At $\beta = 3$, the low SIRs of shadowing variances 6dB and 9dB limit their RB assignments to l_m blocks, which results in their smaller numbers of total RBs than that of 3dB.

The numbers of total RBs for the NOMA scheme are shown in Fig.3(b). (1) When $\beta > 3.5$, the total RB requirements reduce with the increasing path loss exponent. (2) Minimal number of total RBs can be achieved for the back-off factor $\rho = 0.5$ or 0.6. When $\rho < 0.5$, much worse coverage performance is obtained for UE2 [8]. (3) When $\beta \leq 3$, SIRs of both

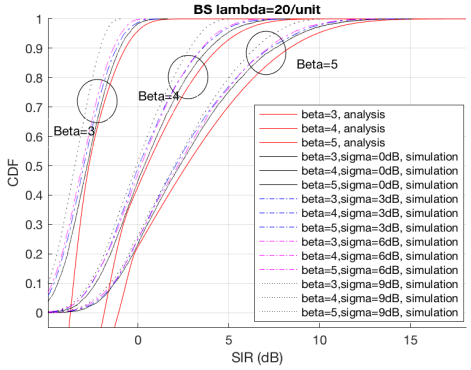

Fig. 2: CDFs of SIR for different shadowing variances and path-loss exponents ($\lambda_b = 20/unit\ area$).

UEs are so small that their RB assignments are always limited to l_m blocks, while RB assignments at $\beta = 3.5$ and 4 partly have this limitation. Hence, the CDF of total RB requirements of the former increase faster than those of the latter. This resource limit leads to smaller numbers of total RBs given an outage rate. (4) Finally, as expected, the numbers of total RBs of all back-off factors are bounded by their corresponding upper bounds.

Thanks to the multiplex mechanism in power domain where two simultaneous transmissions are supported, smaller numbers of total required RBs in NOMA can be obtained in Fig. 3(b) with flexible back-off factors even for a slightly larger l_m in comparison with the OMA scheme in Fig. 3(a). Hence, the NOMA is a preferable access scheme for the 5G and beyond networks even in the dimensioning context.

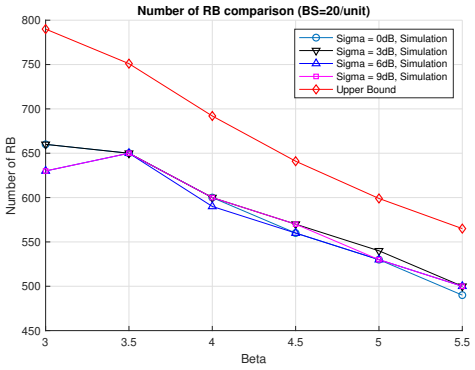

(a) OMA Scheme

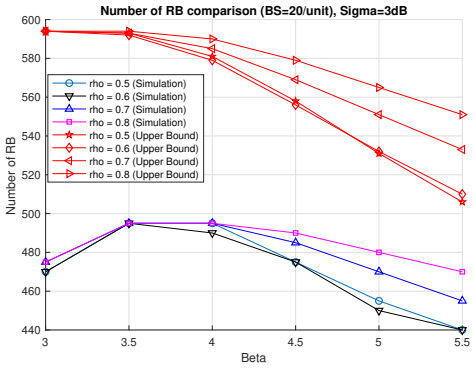

(b) NOMA Scheme

Fig. 3: Number of total RBs and upper bound in function of path-loss exponent to achieve outage rate $\epsilon = 10^{-2}$

VI. Conclusion

In this paper, uplink dimensioning for both OMA and NOMA schemes over shadowing effects is investigated. We first prove that the uplink served UE p.p admits the homogeneous Poisson distribution in the dimensioning context. Then, two SG models for OMA and NOMA schemes are proposed to evaluate numbers of total RBs. These numbers are found to obey compound Poisson distributions. Finally, main simulation results are concluded as follows: (1) Strong shadowing can enhance edge effect and complicate dimensioning. (2) Numbers of total RBs are effectively bounded by upper bounds under different network conditions.

References

[1] T. Bonald and A. Proutiere, "Wireless downlink data channels: User performance and cell dimensioning", in *Proc. ACM MobiCom'03*, San Diego, USA, Sep. 14-19, 2003, pp.39-352.

[2] L. Decreusefond, E. Ferraz, P. Martins, and T. T. Vu, "Robust methods for LTE and WiMAX dimensioning", in *Proc. IEEE Performance Evaluation Methodologies and Tools (VALUETOOLS)*, Corsica, France, Oct. 2012, pp. 74–82.

[3] J-S. Gomez, "Stochastic Models for Cellular Networks Planning and Performance Assessment", Doctoral Thesis, Computer Science, EDITE, tel-01949293, 2018.

[4] B. Blaszczyszyn, M. K. Karry and H. P. Keeler, "Using Poisson Process to Model Lattice Cellular Networks", in *Proc. IEEE InfoCom*, Turin, Italy, 2013, pp. 773-781.

[5] M. K. Karry and M. Jovanovic, "A Queuing Theoretic Approach to the Dimensioning of Wireless Cellular Networks Serving Variable-Bit-Rate Calls", *IEEE Trans. Veh. Tech.*, vol. 62, no.6, pp. 2713-2723, Jul. 2013.

[6] Y. Saito,et al.,"Non-Orthogonal Multiple Access (NOMA) for Cellular Future Radio Access", *Proc. IEEE Veh. Tech. Conference (VTC Spring)*, Dresden, Germany, 2013, pp.1-5

[7] N. Zhang et al.,"Uplink Nonorthogonal Multiple Access in 5G Systems", *IEEE Commun. Lett.*, vol.20, no.3, pp.458-461, Mar. 2016.

[8] Z. Zhang, H. Sun and R. Q. Hu, "Downlink and Uplink Non-Orthogonal Multiple Access in a Dense Wireless Network", *IEEE J. Sel. Areas Commun.*, vol.35, no.12, pp. 2771-2784, Dec. 2017.

[9] T. D. Novlan, H.S. Dhillon, and J.G. Andrews, "Analytical Modeling of Uplink Cellular Networks", *IEEE Trans. Wireless Commun.*, vol.12, no.6, pp.2669-2679, Jun. 2013.

[10] Y. Liang, X. Li and M. Haenggi, "Non-orthogonal Multiple Access (NOMA) in Uplink Poisson Cellular Networks with Power Control", *IEEE Trans. Commun.*, vol.67, issue:11, pp.8021-8036, Nov.2019.

[11] Y. Sun, et al., "On the Performance of Network NOMA in Uplink CoMP Systems: A Stochastic Geometry Approach", *IEEE Trans. Commun.*, vol.67, no.7, pp.5084-5098, Jul. 2019.

[12] Z. Wei, et al., "On the Performance Gain of NOMA Over OMA in Uplink Communication Systems", *IEEE Trans. Commun.*, vo.68, issue:1, pp.536-568, Jan. 2020.

[13] A. S. Marcano and H. L. Christiansen, "Impact of NOMA on Network Capacity Dimensioning for 5G HetNets", *IEEE Access*, vol. 6, pp.13587-13603, Feb. 2018.

[14] F. Baccelli, B. Blaszczyszyn, *"Stochastic Geometry and Wireless Networks, Vol. I"*, Foundations and Trends in Networking, Now Publisher, 2009, 3:3-4

[15] M. Haenggi, "User Point Processes in Cellular Networks", *IEEE Wireless Commun. Lett.*, vol.6, no.2, pp.258-261, Apr. 2017

[16] W. U. Mondal and G. Das, "Uplink User Process in Poisson Cellular Network", *IEEE Commun. Lett.*, vol.21, no.9, pp.2013-2016, Sep. 2017

[17] Y. Wang, M. Haenggi and Z. Tan, "The Meta Distribution of the SIR for Cellular Networks With Power Control", *IEEE Trans. on Commun.* vol.66, no.4, pp. 1745-1757, Apr. 2018

[18] P. Calka, "The distributions of the smallest disks containing the Poisson-Voronoi typical cell and the Crofton cell in the plane", *Advances in Applied Probability*, vol.34, no.4, pp.702–717, 2002.